JOURNAL OF Materials CHEMISTRY

Sonochemical preparation and properties of nanostructured palladium metallic clusters

N. Arul Dhas and A. Gedanken*

Department of Chemistry, Bar-Ilan University, Ramat-Gan, 52900, Israel

Nanoscale particles of palladium metallic clusters have been prepared at room temperature by sonochemical reduction of a 1 : 2 molar mixture of palladium acetate, $Pd(O_2CCH_3)_2$, and myristyltrimethylammonium bromide, $CH_3(CH_2)_{12}N(CH_3)_3Br$ (NR_4X), in tetrahydrofuran (THF) or methanol. Apart from its stabilizing effect, NR_4X acts as a reducing agent, probably due to the decomposition that occurs at the liquid-phase region immediately surrounding the collapsing cavity, and provides reducing radicals. Addition of 0.2 M ethanol–methanol in the THF process enhances the sonochemical reduction of Pd^{II} because of its highly volatile nature producing various reducing radicals inside the collapsing bubble. Analyses by UV–VIS spectroscopy indicated the initial formation of a Pd^{II}–NR_4X complex, which, in turn, reduced to Pd^0. Elemental analysis of the resulting solid (sonication residue) shows that the THF process yields NR_4X stabilized-palladium clusters, whereas the methanol process shows the formation of pure Pd agglomerates. X-Ray diffraction (XRD) and transmission electron microscopy (TEM) with selected area electron diffraction (SAED) techniques were carried out to ascertain the nature, size and morphology of the Pd clusters. TEM of NR_4X stabilized-Pd shows the presence of spherical particles of 10–20 nm in size. Selected area electron diffraction (SAED), along with TEM, reveals that the pure Pd consists of dense agglomerates, whereas NR_4X stabilized-Pd exists as thin crystallites. These Pd nanoclusters are catalytically active towards carbon–carbon coupling, or Heck reaction, in the absence of phosphine ligands, to a moderate extent of 30% conversion. Hydrogenation of cyclohexene to cyclohexane has also been studied using sonochemically generated Pd materials. The catalytic ability of these Pd materials was compared with the commercial Pd on carbon material.

In the past, a flurry of activity has been directed towards the preparation of nanosized noble metallic clusters due to a large enhancement in the catalytic properties of nanoparticles compared to the bulk.[1–6] The smaller the metal particles, the larger the fraction of the metal atoms that are exposed at surfaces, where they are accessible to reactant molecules and available for catalysis. The catalytic activity of the particles generally depends on their size,[3] shape,[4] and stabilizing agents,[5] which are controlled by the preparative conditions. Owing to the diversity of approaches to the design of these nanoscale materials,[7–10] a broad spectrum of physicochemical properties are possible. Synthetic methods such as controlled chemical reduction,[7] photochemical reduction,[8] electrochemical reduction,[9] and metal vaporization[10] have all been used to improve the catalytic properties of palladium. The change in the catalytic activity due to the different preparation conditions, though implied, has not been sufficiently clarified.

Sonochemistry arises from acoustic cavitation phenomenon, that is, the formation, growth and implosive collapse of bubbles in a liquid medium.[11] The extremely high temperatures (> 5000 K), pressures (> 20 MPa), and very high cooling rates ($> 10^7$ K s^{-1}) attained during acoustic cavitation lead to many unique properties in the irradiated solution. Using these extreme conditions, Suslick and his coworkers have prepared amorphous Fe[12] and Mo_2C[13] by using sonochemical decomposition of metal carbonyls in alkane solvent. Adopting a similar technique, we have obtained amorphous Ni by the sonochemical decomposition of nickel tetracarbonyl at ambient conditions.[14] Okitsu *et al.*[15] have prepared Pd nanoparticles in the presence of polymeric surfactants.

Recently, we described a novel *in situ* preparation of carbon-activated palladium nanoparticles by the sonochemical decomposition of a carbon rich organometallic precursor.[16] In a continuation of our studies on noble metallic nanoparticles, herein we describe a simple recipe for the preparation of palladium nanoparticles, using the sonochemical reduction process in non-aqueous medium. The role of simple alcohols, such as ethanol and methanol, on the sonochemical reduction and the choice of solvent on NR_4X stabilization of Pd were studied. Also, we report the catalytic activity of sonochemically prepared Pd nanoparticles, in the hydrogenation of cyclohexene and the C—C coupling or Heck reaction.

Experimental

Materials

All manipulations for the preparations of the sample were performed in an inert-atmosphere box (nitrogen atm, < 10 ppm O_2). Tetrahydrofuran (Bio-Lab, HPLC grade) was distilled over sodium/benzophenone. Methanol and ethanol (Bio-Lab HPLC grade) were used as received. Ultrasonic irradiation was accomplished with a high intensity ultrasonic probe (Misonix XL sonicator; 1 cm diameter Ti horn, 20 kHz, 100 W cm^{-2}).

Synthesis

Ultrasound irradiation of a mixture of 1 : 2 molar ratio of palladium acetate and myristyltrimethylammonium bromide (NR_4X) in THF or methanol yields nanoparticles of palladium. On the addition of NR_4X to a solution of palladium acetate in THF or methanol, strong colour intensification is observed, which indicates the desired interaction between the Pd salt and NR_4X. This may be due to the formation of a NR_4X–Pd^{II} complex.[7] Typically, a solution of $Pd(O_2CMe)_2$ (*ca.* 72 mg) and NR_4X (*ca.* 204 mg) in THF (50 ml) or methanol (50 ml) was sonicated using high intensity ultrasound radiation for three hours by employing a direct immersion titanium horn under argon at a pressure of roughly 0.2 MPa. A round bottom Pyrex glass vessel (total volume 55 ml) was used for the ultrasound irradiation, which had a silicon rubber septum for gas bubbling or sample extraction without exposing the sample to air. The solutions to be sonicated were purged with argon gas, and were kept under argon throughout the experiment. The sonication cell was kept immersed in a cold bath containing a dry ice–acetone mixture during the entire sonication. The resulting black-coloured colloidal solution was taken into

the glove box and carefully transferred into a centrifuge tube. The black powders were recovered by centrifugation (9000 rpm for 30 min), washed thoroughly with THF and ethanol, and dried in vacuum. Dried samples were preserved in vials in an inert-atmosphere glove box for further studies. Ultrasound irradiation using a 0.2 M alcoholic (methanol or ethanol) THF medium was also carried out under similar conditions. The elemental analyses of THF process derived powder shows 26% C, 3.1% H, 1.6% N, 4.1% Br and that of alcoholic THF process derived Pd shows a lower stabilizer content in the sonication product (19% C, 1.9% H, 1.1% N, 2.8% Br). The formation of NR_4X stabilized-Pd is further confirmed by the IR spectrum of the product, which shows the presence of characteristic C—H stretching bands between 2800 and 3000 cm^{-1} of methyl and methylene groups in the 'high frequency region'. On the other hand methanol process-derived Pd shows a negligible amount of carbon (<1%) without N and Br impurities. Upon drying the material in vacuum, highly pyrophoric material is obtained.

Commercially available palladium (10%) supported on carbon (Pd/C, Aldrich) was used as received for the catalytic studies. *In situ* prepared Pd/C nanoparticles were obtained using the procedure described elsewhere.[16] In brief, sonication of a solution of tris-μ-(dibenzylideneacetone)dipalladium (300 mg) in mesitylene (50 ml) under argon for 3 h yields *in situ* Pd/C (*ca.* 55% Pd) nanoparticles. The resulting solid powder was washed thoroughly with THF and ethanol and dried in vacuum prior to the catalytic studies.

To prepare nanostructured pure Pd particles on silica (Pd/SiO_2, 10% Pd), preheated Stobers silica was used. Stobers silica[17] has been prepared by base hydrolysis and condensation of TEOS in an aqueous ethanol medium containing ammonia. A slurry of preheated Stobers silica (100 mg), palladium acetate (200 mg), and NR_4X (400 mg) was irradiated in methanol (50 ml) for 2 h under argon. The resulting solid powder was washed thoroughly with THF and ethanol and dried in vacuum prior to the catalytic studies.

Characterization

The sonochemical reduction of Pd^{II} was followed by UV–VIS spectroscopy with a Varian (model-DMS 100S) spectrophotometer. The X-ray diffraction patterns of Pd nanoparticles were recorded by employing a Rigaku X-ray diffractometer (Model-2028, Cu-Kα). The size of crystallites was calculated from the peak width at a half maximum of (111) X-ray reflection, using the Debye–Scherrer equation.[18] The lattice parameters were calculated with a least-squares fit using the (111), (200), (220) and (311) X-ray reflections. The transmission electron micrographs (TEM) and selected area electron diffraction (SAED) patterns were obtained by employing JEOL-JEM 100SX microscopes. Samples for the TEM examination were prepared by suspending dried samples in dioxane. A drop of the sample suspension was allowed to dry on a copper grid (400 mesh, electron microscopy sciences) coated with carbon film. Samples for elemental analysis were submitted in sealed vials without exposure to air.

Catalysis

In the heterogeneous phase, the activities of different palladium nanoclusters were determined by the hydrogenation of cyclohexene in diethyl ether medium at room temperature. A Pyrex glass reactor was used for the hydrogenation catalytic studies. Typically, 5 mg of Pd was transferred into the reactor in the glove box, without exposing them to air, and were stirred with 5 ml of diethyl ether under high pure N_2 atmosphere for 10 min. Then H_2 gas was bubbled for 10 min and 0.2 ml (*ca.* 2 mM) of cyclohexene was injected through a septum. The reaction mixture was kept under hydrogen atmosphere (*ca.* 0.2 MPa) with stirring for 30 min; then the H_2 supply was detached and the mixture was centrifuged (10 000 rpm). The products were identified by GC and NMR spectroscopy. The conversion (%) was calculated from the GC data. Hydrogenation of cyclohexene using different Pd samples were examined under similar conditions. The time course of the catalytic activity experiments of these Pd powders, in the hydrogenation of cyclohexene, was studied by using 10 mg of Pd, 0.5 ml of cyclohexene in 10 ml of diethyl ether, under similar conditions. During each 10 min interval, 1 ml of the reaction mixture was collected using a septum and was immediately centrifuged. The reaction product was analyzed using a Carbosieve G column with a thermal conductivity detector (TCD). Since different compounds have different TCD responses, correction factors were included in the calculations.

A quartz high pressure reactor was used for the catalytic studies of the carbon–carbon coupling reaction. A mixture of bromobenzene (0.21 ml), styrene (0.23 ml), potassium acetate (235 mg) and 6 mg of Pd powder was placed in a pressure vessel and diluted with dimethylformamide (1 ml). The mixture was heated to 125 °C for 20 h and stirred under argon. The resulting mixture was cooled and filtered. A known amount of internal standard was added to the filtrate and was dissolved in dichloromethane prior to being analyzed by GC.

Results and Discussion

UV–VIS spectra

Sonochemical reduction was considered to be brought about by the reducing radicals generated by ultrasound pyrolysis of the solvent and/or the substances present in the medium. The sonochemical reduction was followed using the UV–VIS absorbance of the Pd^{II}–NR_4X complex. The UV–VIS spectrum of palladium acetate in THF [Fig. 1(a)] shows a strong absorption at 385 nm. Fig. 1(b) shows the absorption spectrum of the reaction mixture (palladium acetate and NR_4X in THF) before irradiation and shows a strong absorption maximum at $\lambda_{max} = 420$ nm corresponding to the Pd^{II}–NR_4X complex. The observed visible absorption band of the Pd^{II}–NR_4X complex is ascribed to the d–d transition of Pd^{II}. The red shift of the visible absorption band of the reaction mixture by the addition of NR_4X [with respect to the palladium acetate in THF ($\lambda_{max} = 385$ nm)] indicates the formation of a palladium acetate–surfactant complex. The intensity of this absorption peak of the Pd^{II}–NR_4X complex gradually decreased with irradiation time. The spectra show a continuous rise in the background towards higher energies, which is due to Mie scattering from the Pd nanoparticles in solution.[19] For comparison, Fig. 2 shows the change in absorption with sonication

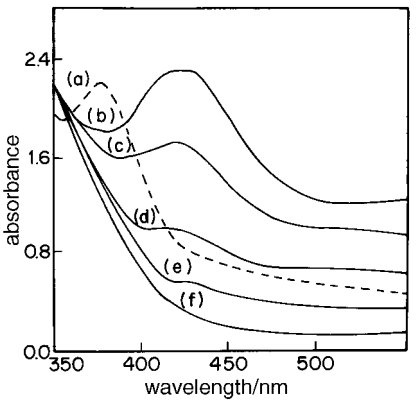

Fig. 1 UV–VIS spectra of: (a) palladium acetate in THF; (b) palladium acetate–NR_4X complex in THF (before irradiation); (c) after 1 h irradiation of (b); (d) after 2 h irradiation of (b); (e) after 3 h irradiation of (b); (f) after 2 h irradiation of the palladium acetate–NR_4X complex in alcoholic THF medium

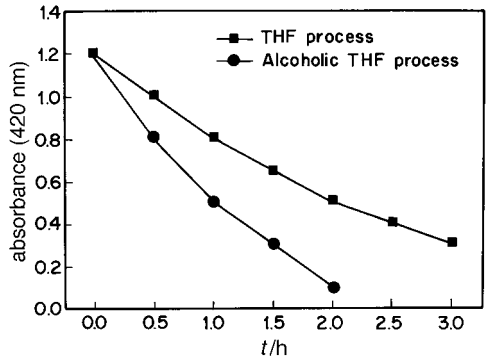

Fig. 2 Plot of absorbance intensity of the 420 nm peak as a function of sonication time. (●) 0.2 M ethanolic THF medium; (■) THF medium.

time, at 420 nm for the complex, in the presence and absence of alcohol. As is clear in both examples, there is a continuous and linear decrease in the Pd^{II}–NR_4X complex concentration during sonication, but the rate of reduction of the complex is enhanced by a factor of 1.5–2 in the presence of alcohol (ethanol or methanol). The linear rate of reduction of Pd^{II} suggests that a constant number of reducing radicals are created per unit time, and the enhanced reduction in the presence of alcohol implies that the production of reducing species is greater in the presence of alcohol. A similar enhanced reduction of Pd^{II} is observed in the methanol process. Therefore, it is evident that the aliphatic alcohols play an important role in determining the rate of nucleation of the metal in solution, as recognized earlier.[20]

Mechanism of sonochemical reduction

The sonochemical reduction of Pd^{II} can be explained by considering the sonochemical reaction site. In the sonochemical process, there are three different regions where the sonochemical reaction can occur,[11] namely: (i) the gas-phase within the collapsing cavity, where elevated temperatures and high pressures are produced; (ii) the thin liquid layer immediately surrounding the collapsing cavity (interfacial region), where the temperature is lower than in the gas-phase reaction zone, but still high enough for a sonochemical decomposition reaction to occur; (iii) the bulk solution at ambient temperatures where reactions take place between solute molecules and the reducing radicals. The low vapor pressure of the Pd^{II} complex eliminates the possibility of the sonochemical reduction taking place in the gas-phase region. The liquid-phase zone and the bulk solution are the regions where the major part of the sonochemical reduction of Pd^{II} to nanosized Pd^0 occurs. It has been well accepted[21] that the long chain surfactants are subjected to pyrolysis by ultrasound irradiation to yield a large variety of reducing radical intermediates such as $^{\bullet}H$, $^{\bullet}CH_3$, $^{\bullet}CH_2R$, *etc.* This pyrolysis event also mainly occurs in the liquid-phase region, not in the gas-phase region, owing to its non-volatile nature. Collapsing of the bubble will aid the dispersion of the radicals. According to Okitsu *et al.*,[15] the following elementary reactions are proposed to explain the mechanism of sonochemical reduction.

$$NR_4X \rightarrow {}^{\bullet}RNR_3X + {}^{\bullet}H \text{ (sonolysis)} \quad (1)$$

$$2\ {}^{\bullet}H + Pd^{II} \rightarrow Pd^0 + 2H^* \quad (2)$$

Okitsu *et al.*[15] have observed a considerable increase in the amount and rate of reduction of Pd^{II} by using excess surfactant (polymers) in aqueous medium. They claim that this is due to the generation of a large number of secondary reducing species in the interfacial region resulting from the attack of H and OH radicals (sonochemical products of water) on the surfactant.

The acceleration in the rate of sonochemical reduction of Pd^{II} in ethanolic–methanolic solution of THF or methanol process may be due to the volatile nature of these alcohols, which can evaporate into the gas-phase region of the collapsing bubble and produce several primary reducing radicals to an even greater extent.[22] Primary radicals are generated through the adiabatic heating of the gas contained in the bubble, as the 'hot spot' theory for cavitation bubble collapse postulates.[11] The reducing radicals generated in the bubble can either recombine or react with the surfactant (NR_4X) in the interfacial region and generate secondary radicals. Consequently, the formation of large amounts of reducing radicals (from the solute and surfactant) accelerates the reduction of Pd^{II} to Pd^0. In general, however, α-hydroxyalkyl radicals are reducing species, that are likely to initiate the reduction process.[23] The primary step for the formation of α-hydroxyalkyl radicals from the aliphatic alcohols may be written as,

$$R'-CH_2OH \rightarrow R'-{}^{\bullet}CHOH + H^{\bullet} \quad (3)$$

A higher concentration of alcohols does not help to enhance the formation of reducing radicals.[22] The sonochemical reduction of a Pd^{II}–NR_4X complex in the presence of simple alcohols is consistent with the following reaction:

$$Pd(CH_3CO_2)_2 \cdot NR_4X + 2R'-{}^{\bullet}CHOH \rightarrow Pd + NR_4X + 2CH_3CO_2H + 2R'-CHO\ (R'=CH_3,\ H) \quad (4)$$

The long chain NR_4X salts formed directly at the reduction center in high local concentration act as very effective protecting agents to keep the particles of freshly reduced metal in solution. The screening of the metal particles by large lipophilic alkyl groups protects the metallic core from agglomeration. It is worth mentioning that the NR_4X stabilized-Pd powders are highly stable and are redispersible without showing any sign of Pd powder segregation. The lack of stabilizing action shown by NR_4X in methanol process is probably due to its high solubility in methanol and therefore yields metallic Pd precipitates.

Powder X-ray studies

Fig. 3 shows X-ray powder diffraction profiles of the studied samples. The XRD pattern of initial stabilized-Pd (THF

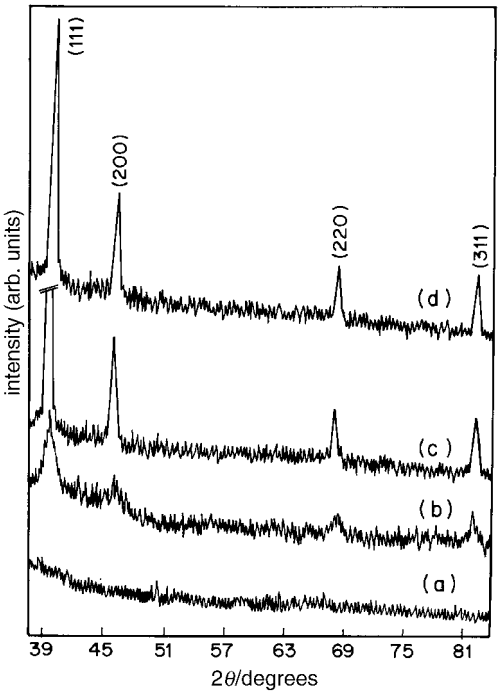

Fig. 3 X-Ray diffractograms of: (a) as-formed Pd (THF process); (b) and (c) calcined (a) at 400 and 600 °C respectively; (d) as-formed Pd (methanol process)

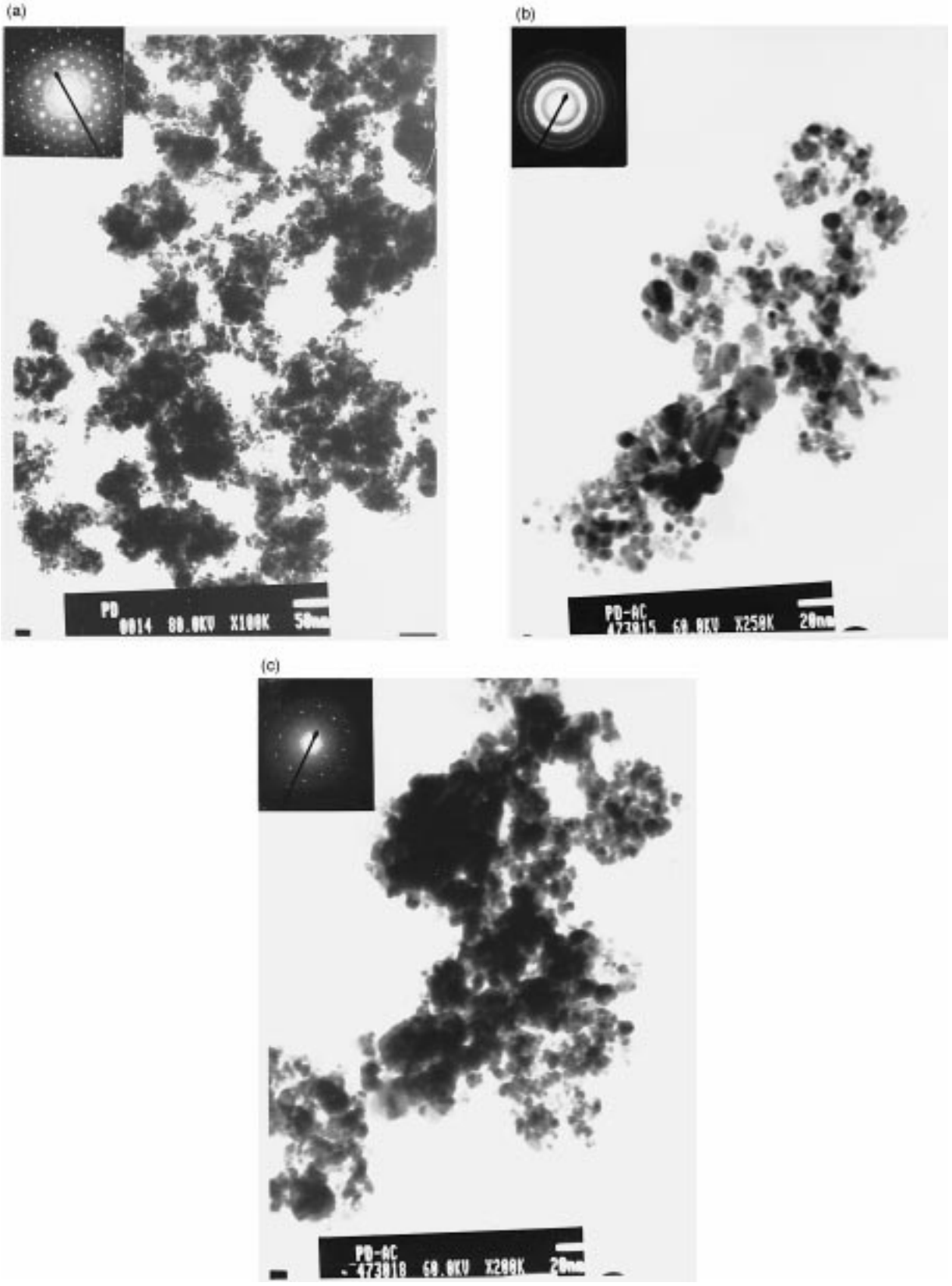

Fig. 4 Transmission electron micrograph and associated SAED pattern (inset) of as-formed Pd: (a) methanol process; (b) THF process; (c) alcoholic THF process

process) is X-ray amorphous [Fig. 3(a)]. The absence of an XRD peak indicated that either the particles were crystallographically amorphous in nature or that the crystalline domains were too small to give rise to crystal reflections in the XRD pattern. However, the nanocrystalline nature of these powders was further confirmed by the SAED pattern, using TEM (see below). The X-ray diffraction peaks of stabilized-Pd are evolved after heating them at 400 and 600 °C under argon for 4 h [Fig. 3(b) and (c)]. The peak positions are consistent with the metallic Pd. The intensity of the XRD reflections are increased with calcination temperature. The increase in the intensity may be due to crystallization of Pd upon heat treatments at higher temperature. The observed sharpening of the X-ray peak upon high thermal treatment is due to the

accompanying particle growth during the secondary crystallization process. The X-ray reflections were indexed on the basis of the fcc structure of Pd with space group *Fm3m* (JCPDS card no. 5-681). The alcoholic THF-derived Pd showed a similar behaviour upon X-ray diffraction after heat treatment. The X-ray diffraction pattern [Fig. 3(d)] of methanol process-derived Pd shows the characteristic diffraction peaks corresponding to Pd^0 without thermal treatment. All possible Pd peaks are present, indicating a polycrystalline nature. The calculated lattice constant $a = 3.8872$ Å is in good agreement with literature values. The average size of crystallites from the X-ray line broadening is 90 and 70 nm for the initial Pd (methanol process) and the crystallized Pd (THF process), respectively. It is gratifying to see that the size of the Pd crystallites by THF process is small, even after crystallization. The relatively large size of the initial Pd derived by methanol process is a direct result of agglomeration, owing to the absence of a protecting agent.

Microstructure

Fig. 4 reveals the TEM microstructure of the palladium nanoparticles. The pure Pd prepared by the methanol process shows [Fig. 4(a)] the presence of irregular particles which are highly agglomerated. The formation of dense agglomerates may be due to the attraction between the nanoparticles, owing to the lack of a stabilizer. The TEM selected area electron diffraction (SAED) pattern of pure Pd nanoparticles shows diffraction spots typical for an agglomerated crystalline material [inset of Fig. 4(a)]. The diffraction pattern could be indexed to an fcc unit cell of dimension $a = 3.8892$ Å. The TEM picture [Fig. 4(b)] of the initial NR_4X stabilized Pd (THF process) shows that the particles are spherical in nature, with a mean diameter of roughly 20 nm. The particles are well separated, without forming an aggregate network on the TEM grid. The SAED pattern of nanoclusters of NR_4X stabilized-Pd (THF process) apparently consists of a ring pattern with diffraction spots [inset of Fig. 4(b)]. The ring pattern is due to diffraction spots from the thin Pd-crystallites. On the other hand, the alcoholic THF-derived NR_4X-stabilized Pd shows [Fig. 4(c)] agglomerates of thin particles. The formation of more aggregated Pd particles in the alcoholic THF medium may be due to the smaller stabilizer (NR_4X) content that promotes the formation of agglomerates. The SAED pattern of alcoholic THF-derived Pd again shows its crystalline nature [inset of Fig. 4(c)]. From the SAED patterns it is evident that both stabilized-Pd are nanocrystalline. From the TEM micrographs it is evident that NR_4X stabilization of Pd clusters allows for particles free of agglomeration. Addition of alcohols enhances the solubility of NR_4X, consequently leading to the formation of a smaller stabilizer content in stabilized Pd or pure Pd (in methanol process) aggregates.

Catalytic activity

The yields of cyclohexane in the hydrogenation of cyclohexene and the *trans*-stilbene in the C—C coupling reaction of as-prepared (before calcination) Pd clusters generated sonochemically are summarized in Table 1. In the hydrogenation reaction, commercial Pd/C shows a 51% conversion of cyclohexene to cyclohexane for 30 min under our experimental conditions. *In situ* prepared Pd/C shows a maximum conversion of *ca.* 86%. The higher catalytic activity towards hydrogenation of cyclohexene may be due to the reactive Pd nanoparticles encapsulated in the amorphous carbon matrix. NR_4X stabilized-Pd (THF process) shows a better conversion compared to that of the commercial one. Pure Pd and Pd/SiO_2 show poor conversion. The poor catalytic ability of pure Pd is due to the fact that aggregation under the experimental conditions prompts drastic loss of catalytic activity. Fig. 5 compares the activity of *in situ* prepared Pd/C and NR_4X stabilized-Pd

Table 1 Catalytic yields of hydrogenation and C—C coupling reaction

material	conversion (%)	
	hydrogenation	C—C coupling
commercial Pd/C	51	20
in situ prepared Pd/C	86	30[a]
NR_4X stabilized-Pd (THF process)	64	25
pure Pd (methanol process)	12	3
pure Pd/SiO_2 (methanol process)	16	9

[a]Ref. 16.

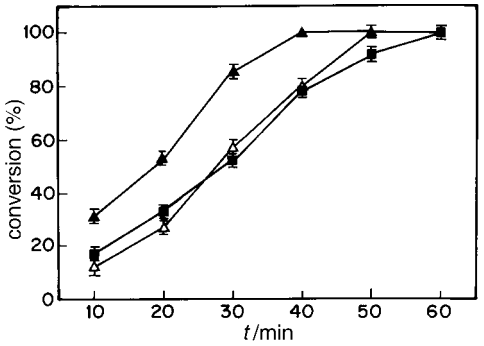

Fig. 5 Catalytic activity of different palladium nanoclusters towards hydrogenation of cyclohexene as a function of time. (■) Commercial carbon activated palladium; (△) NR_4X stabilized palladium prepared by the THF process; (▲) *in situ* prepared carbon activated palladium, see ref. 16.

(THF process) along with commercial Pd/C towards the hydrogenation of cyclohexene. It is very clear that both types of sonochemically prepared Pd show a higher conversion than does the conventional catalyst. It is worth mentioning that the *in situ* Pd/C shows 100% conversion at as little as 40 min.

The catalytic ability of the sonochemically derived palladium nanoparticles was examined in C—C bond forming processes, between bromobenzene and styrene, in the absence of phosphine ligands (Table 1). The catalytic activity of these powders varied with their nature. The commercial Pd/C shows a 20% conversion towards the Heck reaction. *In situ* prepared Pd/C again shows a maximum conversion (30%). The stabilized-Pd (THF process) shows a higher activity (25%) as compared with pure Pd (3% conversion, methanol process). The pure Pd derived from the methanol process shows poor conversion, as expected. Using a higher concentration of NR_4X in the THF process leads to a higher stabilizer content in the resulting powder. However, this poor catalytic activity may be due to the screening of Pd surfaces by a large number stabilizer molecules. It is remarkable that stabilized Pd clusters catalyze the Heck reaction of non-activated bromobenzene, which still represents a synthetic challenge in a practical sense. Indeed, in the case of activated bromoaromatics, these are reported to show poor-to-moderate conversion (5–30%) with Pd colloids.

Conclusion

Sonochemical reduction of Pd^{II} with NR_4X in THF and methanol yields stabilized-Pd and pure Pd, respectively, at room temperature. The *in situ* extraordinarily high temperatures and exceptionally high pressures attained during cavitational collapse, combined with high rates of cooling, lead to the formation of large amounts of reducing radicals which act as reducing agents for the $Pd^{II} \rightarrow Pd^0$ reaction. UV–VIS studies have shown that addition of alcohol in THF or use of a methanol medium remarkably enhances the sonochemical reduction process. The stabilizing agent, NR_4X

freshly generated at the reduction center, helps to keep the Pd nanoclusters free from agglomeration during the THF process. The formation of NR_4X stabilized-Pd with a lower stabilizer content (alcoholic THF process) and pure Pd (methanol process) indicates that the solubility of NR_4X prevents the protective action of NR_4X causing agglomeration. TEM and SAED studies have shown that the stabilized-Pd nanoclusters are nanocrystalline and composed of aggregates of spherical particles of size 10–20 nm. The particle size of 70 nm for stabilized-Pd (X-ray line broadening) indicates a more than three-fold increase in size upon calcination. TEM and SAED results, along with XRD studies of pure Pd, reveal that they are strongly agglomerated and polycrystalline in nature. The formation of crystalline Pd products suggests that an interfacial and/or bulk process is involved in the sonochemical reduction. The catalytic activity of NR_4X stabilized-Pd (THF process) towards hydrogenation and C—C coupling reaction is better than it is with the commercially available Pd/C. From the elemental analyses, TEM images and catalytic studies it is quite evident that the choice of solvent has a direct impact on the chemical composition, aggregation, dispersity and consequently the catalytic activity of the nanoparticles.

This research program was supported by Grant no. 94-00230 from the US–Israel Binational Foundation (BSF), Jerusalem. The authors are grateful to Prof. M. Deutsch, Department of Physics, and Prof. Z. Malik, Department of Life Sciences, for extending their facilities to us. Also, we wish to thank Prof. D. Milstein and Dr Y. Ben-David of the Department of Organic Chemistry at the Weizmann Institute of Science for their encouragement. The authors thank Dr Shifra Hochberg for editorial assistance.

References

1 G. Schmid, *Clusters and Colloids: From Theory to Applications*, VCH, Weinheim, 1994; Y. Volokitin, J. Sinzig, L. J. de-Jongh, G. Schmid, M. N. Vargaftik and I. I. Moiseev, *Science*, 1996, **384**, 621.
2 H. Bonnemann, W. Brijoux and Th. Joussen, *Angew. Chem., Int. Ed. Engl.*, 1990, **29**, 273.
3 J. S. Bradley, E. W. Hill, S. Behal, C. Klein, B. Chaudret and A. Duteil, *Chem. Mater.*, 1992, **4**, 1234.
4 S. Ahmadi, Z. L. Wang, T. C. Green, A. Henglein and M. A. El-Sayed, *Science*, 1996, **272**, 1924.
5 H. Bonnemann and G. A. Braun, *Angew. Chem., Int. Ed. Engl.*, 1996, **35**, 1992.
6 R. F. Heck, *Org. React.*, 1982, **27**, 345; R. F. Heck, *Palladium Reagents in Organic Synthesis*, Academic Press, New York, 1985; Y. Ben-David, M. Portnoy, M. Gozin and D. Milstein, *Organometallics*, 1992, **11**, 1995; M. T. Reetz and G. Lohmer, *Chem. Commun.*, 1996, 1921.
7 H. Bonnemann, W. Brijoux, R. Brinkmann, R. Fretzen, Th. Joussen, R. Koppler, B. Korall, P. Neiteler and J. Richter, *J. Mol. Catal.*, 1994, **86**, 129.
8 Y. Yonezawa, T. Sato, S. Kuroda and K. Kuge, *J. Chem. Soc., Faraday Trans.*, 1991, **87**, 1905.
9 M. T. Reetz and W. Helbig, *J. Am. Chem. Soc.*, 1994, **116**, 7401.
10 G. C. Trivino, K. J. Klabunde and E. B. Dale, *Langmuir*, 1987, **3**, 986.
11 K. S. Suslick (editor), *Ultrasounds: its Chemical, Physical and Biological Effects*, VCH, Weinheim, 1988.
12 K. S. Suslick, S. B. Choe, A. A. Cichowlas and M. W. Grinstaff, *Nature (London)*, 1991, **353**, 414.
13 T. Hyeon, F. Fang and K. S. Suslick, *J. Am. Chem. Soc.*, 1996, **118**, 5492.
14 Y. Koltypin, G. Katabi, R. Prozoroav and A. Gedanken, *J. Non-Cryst. Solids*, 1996, **201**, 159.
15 K. Okitsu, H. Bandow, Y. Maeda and Y. Nagata, *Chem. Mater.*, 1996, **8**, 315.
16 N. Arul Dhas, H. Cohen and A. Gedanken, *J. Phys. Chem. B*, 1997, **101**, 6834.
17 W. Stober, A. Fink and E. Bohn, *J. Colloid Interface Sci.*, 1968, **26**, 62.
18 H. Klug and L. Alexander, *X-Ray Diffraction Procedures*, Wiley, New York, 1962.
19 J. A. Creighton and D. G. Eadon, *J. Chem. Soc., Faraday Trans.*, 1991, **87**, 3881.
20 P. Mulvaney, R. Cooper, F. Grieser and D. Meisel, *J. Phys. Chem.*, 1990, **94**, 8339.
21 A. E. Alegria, Y. Lion, T. Kondo and P. Riesz, *J. Phys. Chem.*, 1989, **93**, 4908.
22 M. Gutierrez and A. Henglein, *J. Phys. Chem.*, 1988, **92**, 2978.
23 J. Z. Sostaric, P. Mulvaney and F. Grieser, *J. Chem. Soc., Faraday Trans.*, 1995, **91**, 2843.

Paper 7/06100E; *Received* 20*th August*, 1997